Color QR Code with Pseudo Quantum Steganography and M-band Wavelet and Patch Group Prior based Denoising

Authors: Julia Yu, Sarah Zhao

School: Danbury Math Academy

Danbury, Connecticut, United States of America

Mentor: Hieu Nguyen

Advisor: Xiaodi Wang

August 2016

All authors made equal contributions to this research project; the names listed above are in alphabetical order

Color QR Code with Pseudo Quantum Steganography and M-band Wavelet and Patch Group Prior based Denoising

Abstract:
As the barcode becomes more widely used, its applications and data capacity demands grow, increasing the need for barcodes with greater data density. Utilizing the quick response (QR) code–one of the many types of barcodes–we developed two algorithms. The first algorithm creates a color QR code that stores more information than a standard QR code and embeds extra data with limited access privilege. The second algorithm denoises a noisy color QR code. These algorithms consist of three techniques: (1) enlarging the data capacity of a compact QR code image by stacking multiple classical QR codes to form a color barcode, (2) embedding information into the color QR code using pseudo quantum signals in an M-band wavelet domain and selecting the discrete 4-band wavelet transforms to compress the QR images, and (3) applying Discrete M-band Wavelet Transform (DMWT) and Patch Group Prior based Denoising (PGPD) methods to denoise noisy QR code images. The peak-signal-to-noise-ratio (PSNR) summary indicates that information in a color QR code can be efficiently stored and retrieved with these methods. Moreover, it shows that our denoising algorithm effectively removes heavy noise from the noisy color QR code. Our algorithms are implemented in a flexible framework, which allows for further modifications to improve both the data capacity of a color QR code and the effectiveness of signal extraction from noisy data to meet future demands.

Keywords: QR Code, M-Band Wavelet Transforms, Pseudo Quantum Signals, Steganography, M-Band Wavelet Denoising, Patch Group Prior based Denoising (PGPD)

Highlights:
In this research, a new color QR code is generated through applying a pseudo-quantum signal embedding algorithm and M-Band wavelet data compression technique. The newly designed color QR code both significantly improves the data capacity from the current black and white QR code and practically incorporates the control of data accessibility through steganography. We also developed a corresponding decoder to denoise and retrieve the information contained in the color QR code with Discrete M-Band Wavelet Transform and Patch Group Prior based Denoising methods with respect to White Gaussian Noise (WGN) and Salt & Pepper Noise (SPN), which are two types of noises commonly considered in image processing [14]. In addition to the usage of steganography, our information embedding algorithm is one of the first that can be employed for the commercial purpose of connecting manufacturer, customer, retail manager, as our QR code can separately carry information for these parties. Secret information can be encrypted into the QR code to function as advertisements, product authenticity checkpoints, and commercial product information. With these applications, our research can shine some light into the considerable potential of such a color QR code in the future economic world.

Table of Contents

I. Introduction and Background
  A. Introduction
    1. Color Barcode
    2. Steganography
    3. Denoising
  B. Background
    1. M-Band Wavelet
    2. Quantum Computing and Pseudo Quantum Signal
    3. Forming the Multicolor QR Code
II. Methods and Results (Part 1): Embedding Secret Information into Color Barcode
  A. Encryption Procedure
  B. Decryption Procedure
  C. Comparing the Original and Extracted Secret Information
III. Methods and Results (Part 2): Denoising a Noisy Color Barcode
  A. Denoising Methods
    1. Discrete M-band Wavelet Transformation (DMWT)
    2. Patch Group Prior Denoising (PGPD)
    3. Combining DMWT and PGPD
  B. Results
IV. Applications
V. Conclusions and Future Research
VI. References

I. Introduction and Background

A. Introduction

The barcode, invented in 1949 by Norman Woodland and Bernard Silver [16], is a machine-readable code that carries data to efficiently track inventory. The barcode's applications continue to revolve around its initial purpose of tracking, but, with increased accessibility to barcode reading applications, barcodes with greater data capacity could evolve from merely tracking products to becoming a 'product-internet' that can quickly link multiple parties together. These advances require the barcode to contain large amounts of data so that it can bridge communications between manufacturers, retailers, and consumers. Thus, we concentrated our pilot project on developing a noise resistant color QR code that stores more data than the black-and-white (BW) QR code. We approached this from three directions: (1) adding color to increase the data capacity, (2) applying steganography to embed secret information into the QR code, and (3) creating a denoising algorithm to remove noise from noisy QR code images.

A.1. Color Barcode

Since its development, barcodes have seen increases in data capacity, particularly with the shift from the 1-D barcode to the 2-D barcode. For the current QR code, the image sizes range from 21 x 21 to 177 x 177 modules [1], and the decoding algorithm can incorporate more colors to increase data storage. Querini *et al.* [2] discussed methods to shift from BW to 4-color and 8-color QR codes. However, the accuracy of decoding algorithms, such as the Reed-Solomon algorithm [3], dramatically decreases when incorporating more colors, and discrepancies between printers, cameras, and scanners lead to even greater difficulty in identifying colors. Thus, we aimed to balance the benefits of increasing the data capacity of the QR code with the disadvantages of adding more colors to decode. In this research, we enlarged QR code capacity through the linear superposition of QR code layers. We tested three color layers, namely the red, green, and blue color channels; however, this procedure can theoretically incorporate more color channels.

A.2. Steganography

After creating a color QR code, a watermark could be embedded to protect its authenticity or provide additional data. However, simply overlaying a signal or image over a QR code could render it unreadable and lessen its data capacity. Instead, we embedded secret information into each channel of our color QR code using pseudo quantum signals in the M-band wavelet domain, which effectively hides the information within the physical QR code. Our embedding process consists of two main steps: (1) the encryption of secret information into an unrecognizable signal and (2) the embedding of the encrypted signal into a color channel of our concatenated QR code with pseudo quantum signals in M-band wavelet domain. If the key to this encryption process is kept private, the embedded information is difficult for outside parties to retrieve, like in standard steganography. However, when the encryption process is based on a public key, this QR code can be used for commercial purposes. To further secure the information in the QR code, pseudo quantum encryption is adopted. Compared to the quantum encryption process, pseudo quantum encryption is a similar system that can be run on both quantum and classical computers. Overall, this pseudo quantum steganography algorithm adds even more data to our color QR code while also regulating access to that information.

A.3. Denoising

The process of creating, printing, and reading a QR code inevitably adds noise; however, increasing error correction within a QR code takes away from the total data capacity of a QR code. Consequently, an effective color QR code decoding algorithm must have an effective denoising procedure in order to maintain a greater data capacity while being readable.

Denoising has two major approaches. The first approach is characterized by obtaining the most important features of the image through data compression and removing noise from the high frequency portion of signals by setting local statistical thresholds, used in wavelet denoising methods by Grace Chang *et al.* [9] and by Portilla *et al.* [10]. The second approach uses a local or non-local pixel or patch group algorithm to model and remove noise from the signals, addressed in many papers including Xu *et al.* [4], Chatterjee and Milanfar [5], and Salmon *et al.* [6]. Despite successes in these two separate denoising approaches, both had significant faults; PGPD, a patch group method, had difficulty denoising the box patterns of the QR code, especially with greater amounts of noise, while wavelet denoising was prone to leaving artifacts. Both approaches decreased contrast between the QR code and its background such that it was difficult to read the QR code even after denoising. Since there does not seem to be any published research combining the trends to create a denoising algorithm that addresses each approach's weaknesses, we developed an M-band wavelet packaged denoising method and combined it with the PGPD method to take advantage of the strengths of both approaches. Then, we compared different methods of denoising QR code images through the Peak Signal to Noise Ratio (PSNR) values and the readability of the denoised code.

We successfully created an RGB color QR code from which we can embed and recover image, audio, and text files. When we relax the number of color channels and define the color-space in a higher dimensional domain, we can improve the color QR code's data capacity within the same size of the original QR code. The details are discussed in the following methods section: (1) Stack multiple color layers reversibly; (2) encrypt and decrypt image and audio messages with pseudo quantum steganography and embed them into QR codes; and (3) extract signal out of noise with DMWT and remove noise from the signals with PGPD.

B. Background

B.1. M-Band Wavelet

Discrete M-band Wavelet Transforms (DMWT) break a k-dimensional signal into M^k different frequency levels with a set of M filter banks, where $M \geq 2$. 2-band wavelets ($M = 2$), such as Daubechies wavelets, are the most commonly used M-band wavelets; however, in this paper, we mainly use 3- and 4-band wavelets constructed in [11]. Let According to

Multiresolution Analysis in [18], a 2-band wavelet lowpass filter bank can be used to form linearly independent vectors to span approximation spaces V_i and highpass filter bank will form detail spaces W_i, and V_i can be decomposed as the direct sum of a higher level approximation subspace V_{i+1} and a detail subspace W_{i+1}: $V_i = V_{i+1} \oplus W_{i+1}$. For example, for Daubechies 4 tap wavelet, $V_0 = \mathbb{R}^{16} = V_1 \oplus W_1 = V_2 \oplus W_2 \oplus W_1 = V_3 \oplus W_3 \oplus W_2 \oplus W_1$. Similarly, the M-band wavelet spans approximation spaces $V_i = V_{i+1} \oplus W^1_{i+1} \oplus W^2_{i+1} \oplus W^3_{i+1}$, where $W^1_{i+1}, W^2_{i+1}, \textit{and } W^3_{i+1}$ are detail subspaces and formed by three highpass filter banks.

In the following, we will use 2-regular 4-band orthonormal wavelet transform as an example to show how DMWT works.

A 2-regular 4-band 2-D wavelet transform decomposes an image into 16 components: one approximation (low frequency) and 15 details (high frequency). The 2-D DMWT of a matrix I is done by multiplying the matrix I by the wavelet transform matrix W on its left and by the transpose of the wavelet transform matrix W^T on its right, written as WIW^T, where $W^T = W^{-1}$ since W is the orthonormal wavelet transform and W^T is the transpose of W.

For an orthonormal M-band wavelet, let $\alpha^{(1)}, \beta^{(1)}, \ldots, \beta^{(M-1)}$ be its filter banks. The filter banks have the following properties: (1) $\|\alpha\| = \ldots = \|\beta^{(1)}\| = \ldots = \|\beta^{(M-1)}\| = 1$, (2) $\sum_{i=1}^{N} \alpha_i = \sqrt{M}$, $\sum_{i=1}^{N} \beta_i^{(m)} = 0$, and (3) $\alpha \bullet \beta^{(m)} = 0$, for $m = 1, \ldots, M-1$, where N is the length of each filter bank. For $K \geq 2$, K-regular orthonormal M-band wavelets have the additional K-vanishing moment property: $\sum_{i=1}^{N} i^j \bullet \beta_i^{(m)} = 0$ for $m = 1, \ldots, M-1$, $j = 0, 1, \ldots, K-1$. An example of a 2-regular 4-band 16 by 16 wavelet transform matrix W is shown below:

<table>
<tr><td>α=[-0.067371764, 0.094195111, 0.40580489, 0.567371764, 0.567371764, 0.40580489, 0.094195111, -0.067371764]</td><td rowspan="4">$\begin{bmatrix} \alpha_1 & \alpha_2 & \alpha_3 & \alpha_4 & \alpha_5 & \alpha_6 & \alpha_7 & \alpha_8 & 0 & 0 & 0 & 0 & 0 & 0 & 0 & 0 \\ 0 & 0 & 0 & 0 & \alpha_1 & \alpha_2 & \alpha_3 & \alpha_4 & \alpha_5 & \alpha_6 & \alpha_7 & \alpha_8 & 0 & 0 & 0 & 0 \\ 0 & 0 & 0 & 0 & 0 & 0 & 0 & 0 & \alpha_1 & \alpha_2 & \alpha_3 & \alpha_4 & \alpha_5 & \alpha_6 & \alpha_7 & \alpha_8 \\ \alpha_5 & \alpha_6 & \alpha_7 & \alpha_8 & 0 & 0 & 0 & 0 & 0 & 0 & 0 & 0 & \alpha_1 & \alpha_2 & \alpha_3 & \alpha_4 \\ \beta_1 & \beta_2 & \beta_3 & \beta_4 & \beta_5 & \beta_6 & \beta_7 & \beta_8 & 0 & 0 & 0 & 0 & 0 & 0 & 0 & 0 \\ 0 & 0 & 0 & 0 & \beta_1 & \beta_2 & \beta_3 & \beta_4 & \beta_5 & \beta_6 & \beta_7 & \beta_8 & 0 & 0 & 0 & 0 \\ 0 & 0 & 0 & 0 & 0 & 0 & 0 & 0 & \beta_1 & \beta_2 & \beta_3 & \beta_4 & \beta_5 & \beta_6 & \beta_7 & \beta_8 \\ \beta_5 & \beta_6 & \beta_7 & \beta_8 & 0 & 0 & 0 & 0 & 0 & 0 & 0 & 0 & \beta_1 & \beta_2 & \beta_3 & \beta_4 \\ \gamma_1 & \gamma_2 & \gamma_3 & \gamma_4 & \gamma_5 & \gamma_6 & \gamma_7 & \gamma_8 & 0 & 0 & 0 & 0 & 0 & 0 & 0 & 0 \\ 0 & 0 & 0 & 0 & \gamma_1 & \gamma_2 & \gamma_3 & \gamma_4 & \gamma_5 & \gamma_6 & \gamma_7 & \gamma_8 & 0 & 0 & 0 & 0 \\ 0 & 0 & 0 & 0 & 0 & 0 & 0 & 0 & \gamma_1 & \gamma_2 & \gamma_3 & \gamma_4 & \gamma_5 & \gamma_6 & \gamma_7 & \gamma_8 \\ \gamma_5 & \gamma_6 & \gamma_7 & \gamma_8 & 0 & 0 & 0 & 0 & 0 & 0 & 0 & 0 & \gamma_1 & \gamma_2 & \gamma_3 & \gamma_4 \\ \delta_1 & \delta_2 & \delta_3 & \delta_4 & \delta_5 & \delta_6 & \delta_7 & \delta_8 & 0 & 0 & 0 & 0 & 0 & 0 & 0 & 0 \\ 0 & 0 & 0 & 0 & \delta_1 & \delta_2 & \delta_3 & \delta_4 & \delta_5 & \delta_6 & \delta_7 & \delta_8 & 0 & 0 & 0 & 0 \\ 0 & 0 & 0 & 0 & 0 & 0 & 0 & 0 & \delta_1 & \delta_2 & \delta_3 & \delta_4 & \delta_5 & \delta_6 & \delta_7 & \delta_8 \\ \delta_5 & \delta_6 & \delta_7 & \delta_8 & 0 & 0 & 0 & 0 & 0 & 0 & 0 & 0 & \delta_1 & \delta_2 & \delta_3 & \delta_4 \end{bmatrix}$</td></tr>
<tr><td>β=[-0.094195111, 0.067371764, 0.567371764, 0.40580489, -0.40580489, -0.567371764,-0.067371764, 0.094195111]</td></tr>
<tr><td>γ=[-0.094195111, -0.067371764, 0.567371764, -0.40580489, -0.40580489, 0.567371764,-0.067371764, -0.094195111]</td></tr>
<tr><td>δ=[-0.067371764, -0.094195111,0.40580489, -0.567371764, 0.567371764, -0.40580489,0.094195111, 0.067371764]</td></tr>
</table>

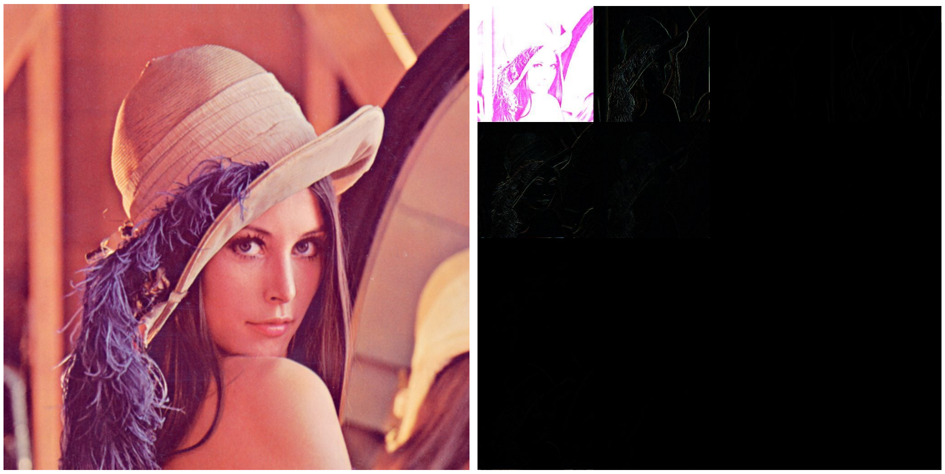

Figure 1: Sample of 4-Band Wavelet Transformation;
the approximation component can be seen in the top left corner of the image on the right

B.2. Quantum Computing and Pseudo Quantum Signal

A quantum computer utilizes quantum properties to make computations, utilizing qubits instead of classical bits to store data. While a classical bit can only have one of two states, 0 or 1, a qubit can be in any linear combination of the states $|0\rangle = [1,0]^T$ and $|1\rangle = [0,1]^T$.

The state of any one qubit can be written as $|\psi\rangle = \alpha|0\rangle + \beta|1\rangle$, where $|\alpha|^2 + |\beta|^2 = 1$ and α and β are complex numbers, which defines a point on the 3-D unit sphere. (The state of a qubit ψ can also be written as $|\psi\rangle = cos(\theta/2) * |0\rangle + e^{i\varphi} sin(\theta/2) * |1\rangle$, where θ and φ are real numbers. There are infinitely many such points. [13]

From some signal $S = \{s_i\}_{i=1}^{n}$, a pseudo quantum signal can be derived – we define a linear transformation F such that $F(s^*) = m\pi/3$ and $F(s_*) = m\pi/6$, with $s^* = max(s_i)$, $s_* = min(s_i)$, and $m \in \mathbb{N}$, which transforms S into the interval $[m\pi/6,\ m\pi/3]$ with $\theta_i = F(s_i)$ for $i = 1, 2, ...n$. The transformed result, which we call $F(S)$, consists of angles, expressed as θ_i, which can be used to define pseudo qubits, expressed as $|s_i\rangle = cos\theta_i|0\rangle + sin\theta_i|1\rangle$. The transformation F is defined as a "pseudo quantum signal converter" through which a classical signal can be transformed into a pseudo quantum signal, while the state of each individual qubit is called a "pseudo quantum signal" [7] [8].

This pseudo quantum signal can be processed by classical computers to simulate quantum computing processes; hence, we have utilized these pseudo quantum signals to embed secret information as though through a quantum computer.

B.3. Forming the Multicolor QR Code

In order to increase the capacity of the QR code, we reversibly stacked three color layers. Utilizing an online QR code generator, we converted text files into QR codes and defined an R^3 color space as shown in Figure 2. All other colors can be spanned by the linear combination of Red ([1,0,0]), Green ([0,1,0]), and Blue ([0,0,1]) colors with 0 to 255 scales of intensity. The nature of RGB being orthonormal color base vectors allows a color QR code to be split into red, green, and blue QR images accurately and to be stacked from different QR images on these three color channels.We can generalize this idea to stack more color layers to further increase the data capacity of the QR code.

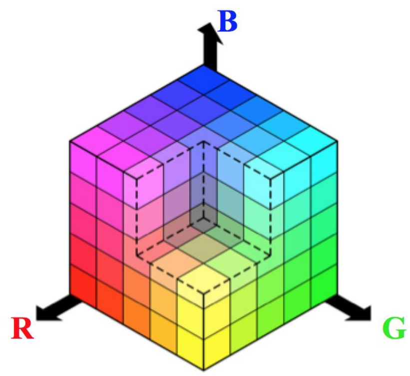

Figure 2. Red ([1,0,0]), Green ([0,1,0]), and Blue ([0,0,1]) spanning an R^3 color space [15]

II. Methods and Results (Part 1): Embedding Secret Information into Color Barcode

After the 3-color QR code is split into its RGB color channels, we can obtain three 2-D QR codes, one from each color channel. We then embed additional secret information into these channels with the pseudo quantum steganography algorithm. For our example, we embedded an image, an audio file, and another barcode inside our color barcode.

A. Encryption Procedure

1. Wavelet Transform: Perform wavelet transformation on each channel of the color barcode to obtain the approximation portion, $T = WIW^{-1}$, where T is the wavelet transformed image matrix, W is the wavelet matrix, and I is the barcode.

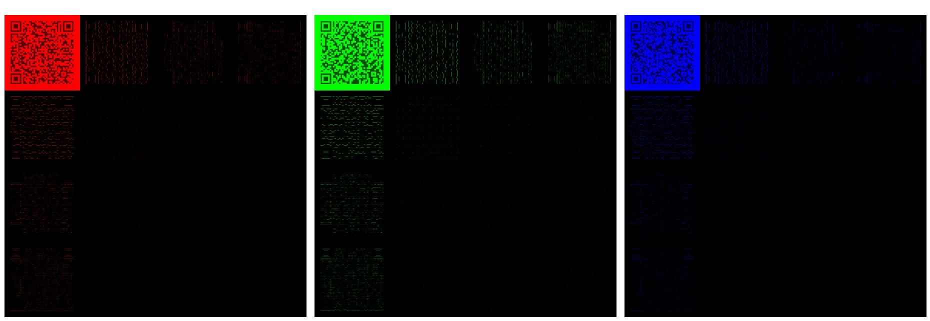

Figure 3: Approximation (in top left corner of each image) and details of the RGB color channels after performing DMWT

2. <u>Quantum Steganography</u>: With a quantum computer, we can generate random qubits such that:

$$\left|S_{ij}\right\rangle = P_{ij_1}\left|0\right\rangle + P_{ij_2}\left|1\right\rangle,$$

where S_{ij} is the qubit corresponding to each index of the approximation portion.

After acquiring the qubits, we can start embedding each index of the secret information to the corresponding index of the approximation portion using:

$$\theta_{E,ij} = m\begin{Bmatrix} \cos^{-1}(\cos(\frac{\theta_{ij}}{m}) + \varepsilon\cos(\frac{\alpha_{ij}}{n})), & \left|P_{ij1}\right| \geq \left|P_{ij_2}\right| \\ \sin^{-1}(\sin(\frac{\theta_{ij}}{m}) + \varepsilon\sin(\frac{\alpha_{ij}}{n})), & \left|P_{ij_1}\right| < \left|P_{ij_2}\right| \end{Bmatrix}$$

3. <u>Pseudo Quantum Steganography</u>: As mentioned earlier, we are proposing a steganography method called Quantum Signal Embedding. This method can be achieved with a quantum computer. However, since a classical computer cannot generate a true qubit, we mimic a quantum bit with "Pseudo Quantum Signals." In order to perform this method, we first transform the approximation portion and the secret information into pseudo quantum signals (angles) using the following linear transformations:

$$\theta_{ij} = f(A_{ij}) = \frac{m\pi(A_{ij} + \mu_1 - 2\nu_1)}{6(\mu_1 - \nu_1)}, \text{ where } \mu_1 = \max(A_{ij}), \nu_1 = \min(A_{ij}). \frac{m\pi}{6} \leq \theta \leq \frac{m\pi}{3}$$

$$\alpha_{ij} = f(X_{ij}) = \frac{n\pi(X_{ij} + \mu_2 - 2\nu_2)}{6(\mu_2 - \nu_2)}, \text{ where } \mu_2 = \max(X_{ij}), \nu_2 = \min(X_{ij}). \frac{n\pi}{6} \leq \alpha \leq \frac{n\pi}{3}$$

where θ is the pseudo quantum signal angle vector of the approximation portion A of the wavelet transformed matrix, and α is the pseudo quantum signal angle vector of the secret information X.

Using the idea of the uncertainty and randomness of the qubit, we create K using a random number generator from a classical computer, and k_{ij} is any number between and including 0 and 1. Now, we can perform Pseudo Quantum Signal Embedding as the following:

$$\theta_{E,ij} = m\begin{Bmatrix} \cos^{-1}(\cos(\frac{\theta_{ij}}{m}) + \varepsilon\cos(\frac{\alpha_{ij}}{n})), & k_{ij} \geq 0.5 \\ \sin^{-1}(\sin(\frac{\theta_{ij}}{m}) + \varepsilon\sin(\frac{\alpha_{ij}}{n})), & k_{ij} < 0.5 \end{Bmatrix}$$

, where ε is the embedding intensity.

Once completed, we do the inverse of linear transformation as performed earlier to obtain the embedded approximation portion.

$$A_{E,ij} = \frac{6\theta_{E,ij}(\mu_1 - \nu_1)}{m\pi} - \mu_1 + 2\nu_1$$

4. Inverse Wavelet Transform: Replace the embedded approximation portion to the wavelet transformed matrix to obtain T_E and perform the inverse wavelet transformation to obtain the embedded color barcode: $I_E = W^{-1} T_E W$.

Figure 4: Original (left) and Embedded (right) Color QR code

B. Decryption Procedure

As shown from the section above, the embedded color QR code and the original QR code have a high similarity. Therefore, when the embedded color barcode is being scanned, the information is exactly the same as the original ones. Once the receiver obtains the codebook, the following procedure extracts the secret information as follows:

1. Obtain the Pseudo Quantum Signals Approximations: Construct a copy of the original color barcode after scanning the embedded barcode. Then, after the wavelet transform, we take the approximation portions from each barcode wavelet domain and apply pseudo quantum signal linear transformation to both barcodes to obtain angles θ and θ_E. [see steps 1 and 3 from encryption procedure]

2. Extract Secret Signals: With the embedded pseudo quantum signal approximation portion(θ_E) and the original pseudo quantum signal approximation (θ), the extraction of secret information follows:

$$\alpha_{ij} = n \begin{Bmatrix} \cos^{-1}\left(\dfrac{\cos(\frac{\theta_{E,ij}}{m}) - \cos(\frac{\theta_{ij}}{m})}{\varepsilon}\right), & k_{ij} \geq 0.5 \\ \sin^{-1}\left(\dfrac{\sin(\frac{\theta_{E,ij}}{m}) - \sin(\frac{\theta_{ij}}{m})}{\varepsilon}\right), & k_{ij} < 0.5 \end{Bmatrix}$$

<u>3. Obtain Secret Information</u>: α is the secret information in the form of pseudo quantum signals. To get the secret information, we use the inverse of linear transformation which was performed during the encrypting procedure.

$$\text{Extracted\_secret}_{\text{ij}} = \frac{6\alpha_{\text{ij}}(\mu_2 - \nu_2)}{\text{n}\pi} - \mu_2 + 2\nu_2$$

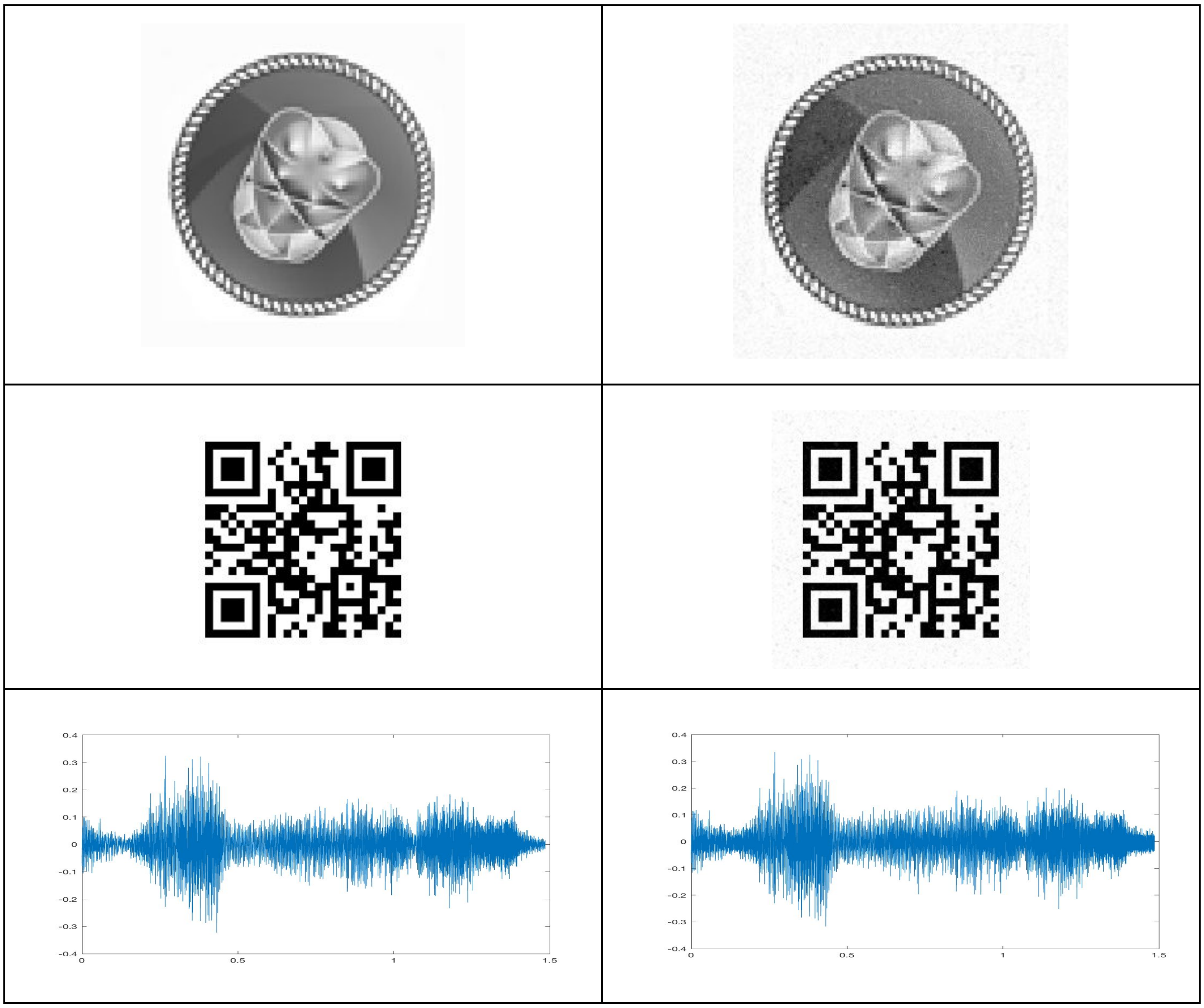

Figure 5: Original (left) and Extracted Secret Information (right) when $\varepsilon = 0.01$

C. Comparing the Original and Extracted Secret Information

Peak Signal-to-Noise Ratio (PSNR) is commonly used to compare the reconstructed image and the original image. Hence, we use PSNR to determine the quality, robustness, and similarity of the extracted secret information compare to the original secret information.

First, we calculate the Mean Squared Error (MSE):

$$MSE = \frac{1}{mn} \sum_{i=1}^{m} \sum_{j=1}^{n} (I_{E,ij} - I_{ij})^2$$
,

where I_E is the extracted image and I is the original image.

PSNR is used for image measurement. For audio, we need to use Signal-to-Noise Ratio (SNR) to observe the ratio between the noise level and the signal level.

We also used Relative Similarity (RS) to measure the exactness between the original and the embedded color barcodes. Below are the formulas for RSNR, RS, and SNR:

$PSNR = 10 \cdot \log(\frac{255^2}{MSE})$	$RS(I_2, I_1) = 1 - \frac{\lVert I_2 - I_1 \rVert_1}{\lVert I_1 \rVert_1}$	$SNR = 10\log\left\{\frac{\sum_{a=1}^{M_t} Z^2(a)}{\sum [Z(a) - Z^*(a)]^2}\right\}$

	PSNR (of extracted secret information) / RS (of embedded and original barcodes)		
Intensity Indicator (ε)	Secret QR Code	Siemens Logo	Audio(SNR)
.0025	16.00/.8600	16.61/.8613	-6.9946
.005	23.67/.8622	22.18/.8641	-1.5020
.010	32.68/.8660	30.67/.8689	7.8280
.020	30.23/.8740	31.81/.8795	13.6336
.025	16.2391/.8759	17.9402.8821	5.3083

Table 1: PSNR, RS, and SNR values of the secret information on different intensity indicator

Observed from table above, the intensity indicator should be neither too small nor too large. Negative SNR values indicate that there is more noise than signal. For example, with the 0.0025 and 0.05 intensity indicator values, the secret audio information could not be recognizable due to a high noise to signal ratio. From our results, it seems that between 0.010 and 0.025 is the best range for the intensity indicator ε to obtain a great extraction result.

III. Methods and Results (Part 2): Denoising a Noisy Color Barcode

A. Denoising Methods

In general, image denoising aims to obtain an estimate of an original $m \times k$ image $F = \{f[i,j]\}$ from the contaminated image $C = \{c[i,j]\}$, which is defined by:

$$c[i,j] = f[i,j] + n[i,j], \text{ for } i \in [1,m] \text{ and } j \in [1,k] ,$$

where {n[i,j]} is noise that is independently and identically distributed (*iid*) as normal $N(0, \sigma_n^2)$ and independent of the original image. The closer the estimate $F' = \{f'[i,j]\}$ is to the original image *F*, the smaller the value of the Mean-Square Error (MSE) and the larger the value of the Peak Signal to Noise Ratio (PSNR). We will compare the denoising methods with PSNR.

A.1. Denoising with the Wavelet Toolbox

Utilizing the Wavelet Toolbox in MATLAB, we are able to use built-in 2-band wavelets, such as Daubechies wavelets, to denoise a noisy barcode. When testing various denoising methods, we compared the results of denoising in the Wavelet Toolbox to the results of denoising with just M-band wavelets (process described in A.2.). We generally found that the M-band wavelets yielded clearer results than the Wavelet Toolbox; additionally, M-band wavelet denoising were less prone to introducing the image distortions seen when using the Wavelet Toolbox. Between the two methods, only the M-band wavelet denoising yielded results that could be read by a phone reader.

A.2. Discrete M-band Wavelet Transformation (DMWT)

Wavelet image denoising utilizes wavelet transform, which concentrates image features into a few large-magnitude wavelet coefficients. The smaller wavelet coefficients are likely to be noise that can be either diminished or removed without affecting the image quality. Wavelet transform decomposes an image into one lower frequency subband (approximation portion), which contains most of the image information and energy, and high frequency subbands (details), which contain most of the noise information. We modify VisuShrink universal threshold proposed by Donoho and Johnstone [17] by setting $T = \sigma \sqrt{2 ln\, K}$ where σ is the noise variance of the original noisy image and *K* is the size of this image. We can then apply hard thresholding to these details to remove noise.

Instead of using the traditional 2-band wavelets, we chose to use M-band wavelets, where $M > 2$, for denoising because M-band wavelets are more efficient in quickly separating the image into a better approximation and details. We added heavy noise to the color QR code RGB channels and tested our DMWT packaged image denoising with 2-regular 3-band, 2-regular 4-band, and 4-regular 4-band wavelets.

Since the process is similar across the M-band wavelets, we will use the 4-band wavelet transform package to demonstrate our package algorithm. The package applies 4-band wavelet transform to the $4^n \times 4^n$ noisy barcode image *C*, resulting in one approximation (*A*) and 15 details ($D_1, D_2, \ldots, D_{15}$). We then perform DMWT on the fifteen $4^{n-1} \times 4^{n-1}$ resulting details, separating each D_i into sixteen $4^{n-2} \times 4^{n-2}$ portions (D_i's approximation and 15 details) – let D'_i be the resulting wavelet transformed D_i. After doing so, we set a local hard threshold $T_{ij} = \sigma_{ij}\sqrt{2ln\, 4^{\,n-2}}$ on each of the 15 details of each $D_i{}'$ (for $i, j = 1, \ldots, 15$) to remove noise and we then perform inverse wavelet transform on denoised version of D_i' to get denoised version of D_i : $D_{i\ denoised} = W^T D_i' W$. Our package then replaces the original details D_i with the denoised ones $D_{i\ denoised}$. Finally, we perform inverse wavelet transform once more to display the final denoised image.

A.3. Patch Group Prior based Denoising (PGPD)

The second method that we incorporated was the Patch Group Prior based Denoising (PGPD) method from Xu *et al.* [4]. This method follows the second approach of denoising: using a patch-based algorithm to model and remove noise. First, the prior learning stage trains the Patch Group Gaussian Mixture Model (PG-GMM) to learn a set of Gaussians from a number of training Patch Groups. Then, the denoising stage forms patch groups of similar patches and subtracts the mean of the group from each. Finally, it selects the most suitable Gaussian component from the trained PG-GMM for each patch group and takes the orthonormal matrix of eigenvectors from the singular value decomposition of its covariance matrix. This matrix is then used in weighted sparse coding and the patch group is denoised. After this process is completed for each patch group, all the groups are reassembled to form the complete denoised image [4].

A.4. Combining DMWT with PGPD

When testing the two different methods, we noticed that both methods had their strengths and weaknesses. DMWT, which transforms the image to different frequency domains and removes noise in the high frequency portions, succeeds in denoising a QR code image with heavy noise such that it can be read by the QR decoder app. However, DMWT fails to remove the white noise on the white border of the QR code. On the other hand, PGPD successfully removes white noise in the white areas of the barcode, but has great difficulty denoising heavy noise. Combining the two methods resulted in better denoised color QR code images.

B. Results

1. The maximum difference between the QR image matrices before and after the color channel stacking or splitting is zero. Therefore, the linear superposition of three QR codes to form an RGB QR code can be stacked and retrieved accurately.
2. For any single color channel, the QR code is attacked with noise (Gaussian noise with mean of zero and variances of 0.01 and 0.1; salt and pepper noise with variances of 0.1 and 0.2) to be used for the evaluation of the denoising results. Figure 7 summarizes the PSNR values for the DMWT (M = 2, 3, 4) and the PGPD methods. The PSNR results for 2-, 3-, and 4- band wavelet transform and PGPD methods for WGN with variance of 0.01 are shown in Figure 7a. In general, the PGPD method (Figure 7b and 7d) returns a higher PSNR value than those resulting from DMWT denoising (Figure 7a and 7c). The combination of PGPD and DMWT often returned values with lower PSNR values than that from just performing PGPD; however, with noise that was a little heavier like Gaussian(0,0.1), the combination of discrete 2-regular 4-band wavelet transform followed by PGPD (2R4B-PGPD), in Figure 7c, returned a higher value than any of the other methods.

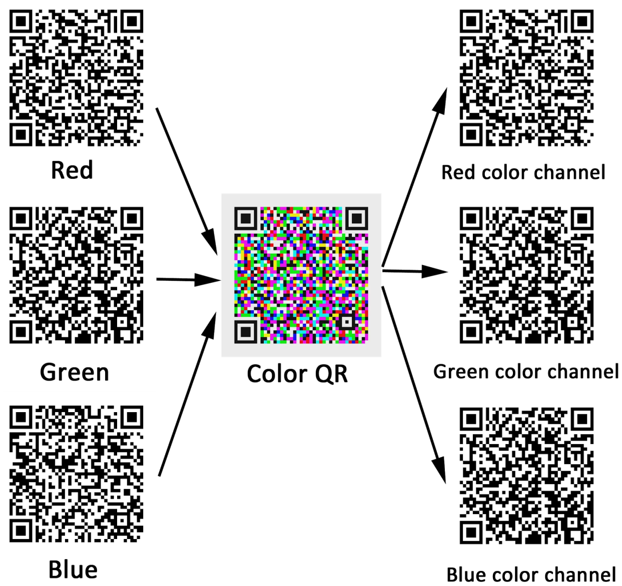

Figure 6: The reversible stacking and retrieval of QR codes

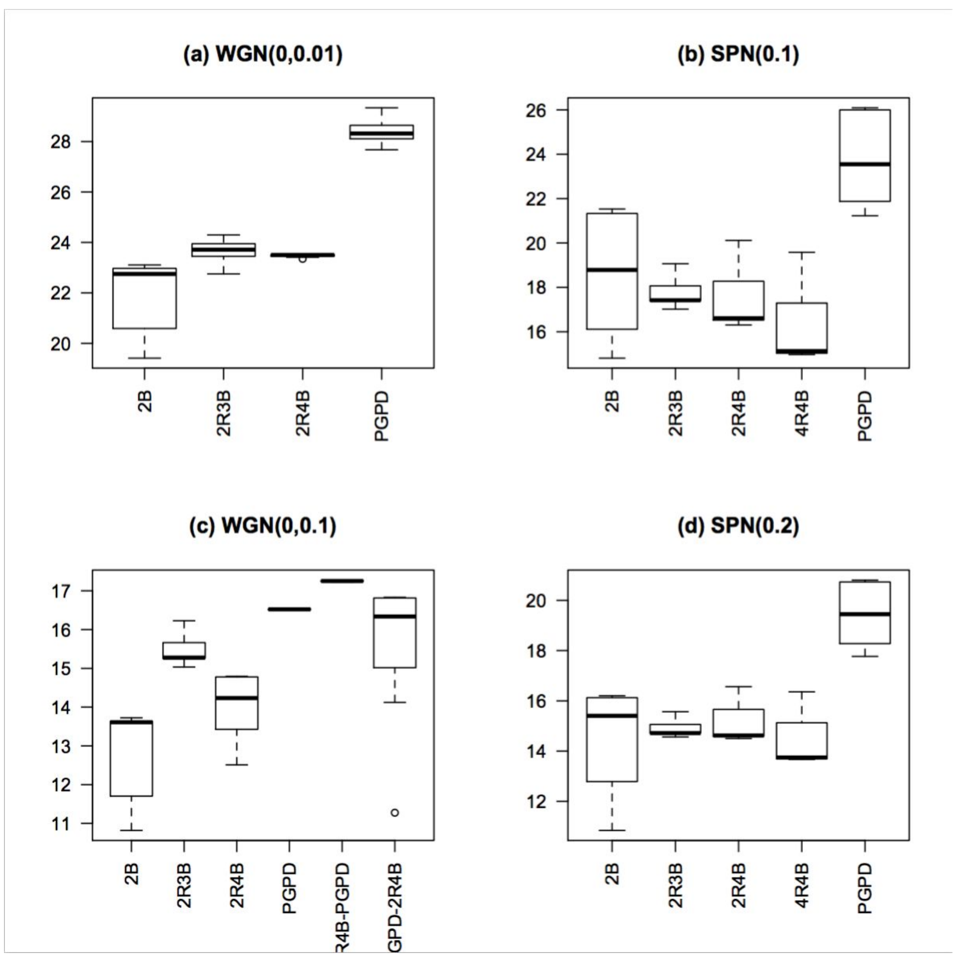

Figure 7: PSNR values of DMWT and PGPD methods with Gaussian and Salt & Pepper noise

When noise is heavy, such as WGN with mean 1 and variance 1, the DMWT method performs better than PGPD, as DMWT renders the previously unreadable barcode image readable by the QR code scanner app while PGPD fails. The noisy QR code and the resulting images denoised by DMWT, PGPD, and the DMWT-PGPD are shown in Figure 8. When the noise is heavy, DMWT-PGPD not only can recover an image with a higher PSNR than the results of either DMWT or PGPD alone, but also can produce a QR code image from which the QR code scanner app can retrieve information accurately.

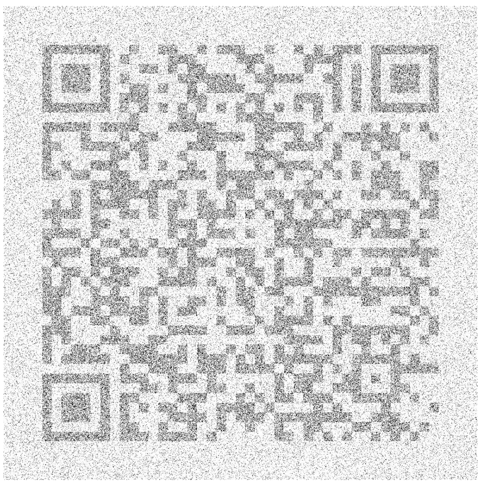

Original Gaussian(1,1) noisy Image
Not able to be read by QR code scanner app

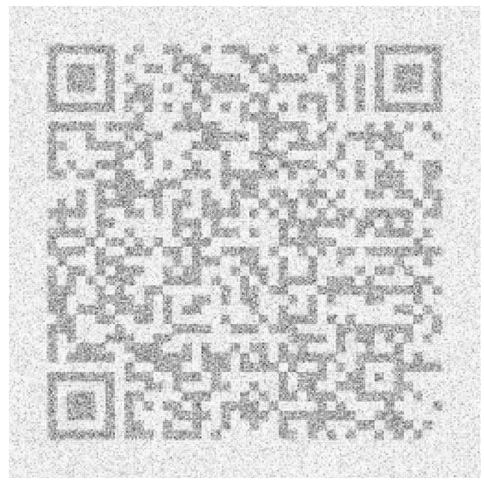

2-regular 4-band Wavelet Denoised
Able to be read by QR code scanner app

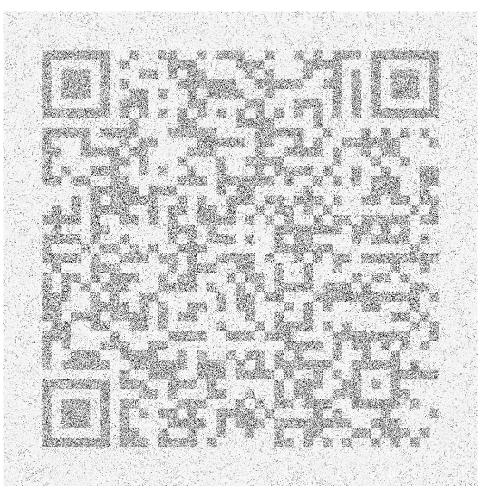

PGPD Denoised
Not able to be read by QR code scanner app

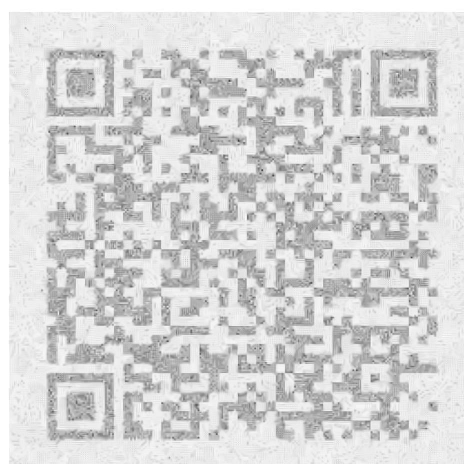

2-reg 4-band wavelet – PGPD denoised
Able to be read by QR code scanner app

Figure 8: Noisy QR code image and resulting denoised images from DMWT, PGPD, and DMWT-PGPD

IV. Applications

We present a 3-color QR code (Figure 9) that can be used to assist future enterprises by linking the manufacturers, consumers, and retailers. In this example, the red layer QR code and its embedded reward allows a manufacturer to track and advertise its product. The green layer QR code and its encrypted company logo image enable a consumer to check the authenticity of the product with a manufacture key provided on receipt after purchase and explore more products from the URL. Finally, the blue layer QR code allows the retailer to track sales and encrypt additional messages for readers of the code.

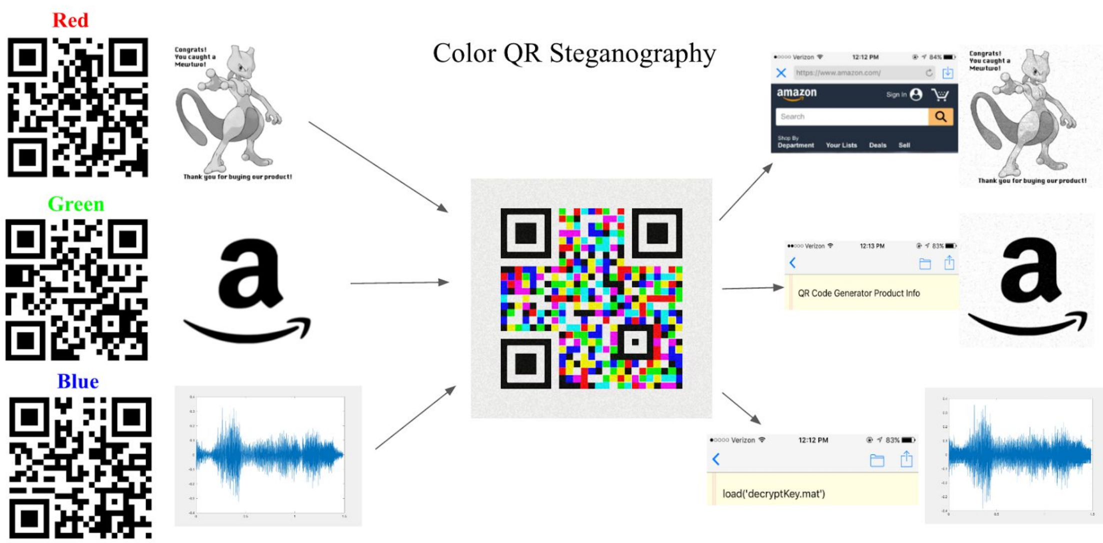

Figure 9: Future Enterprise Model

V. Conclusions and Future Research

The main features of the color QR code generator are increased data capacity by reversibly stacking multiple classical QR codes and pseudo quantum steganography. The color QR code decoder includes denoising, which combines the DMWT and PGPD denoising methods to remove noise and return an unreadable barcode into a readable state. In summary, our color QR code generator and decoder work to store greater amounts of public and private information into the same physical space as the classical black and white QR code. Our barcode can advertise products and provide these products' information for the consumer's convenience. Combined with a checkout key from the manufacturer with which to decode embedded information, our color QR code can even verify the authenticity of products and summarize sales management data. With a color QR reader app, manufacturers, retailers, and consumers can exchange information on a product in a quick, accurate manner through a small product-specific network.

The potential of the color QR code is great. However, some obstacles must be overcome before such potential can be realized. In particular, the development of a more time-efficient denoising algorithm with equal effectiveness at denoising would be necessary for a color QR code to become widely used. Current barcodes, such as the regular 1-D barcode and the classical QR code, can be swiftly read and denoised by machines, contributing to their proliferation as a product. Similar speed must be achieved in the reading of the color QR code, whether through improved hardware or through more efficient algorithms. Additionally, in order to create a viable decoder application for this color QR code, we would have to investigate the denoising of other kinds of noise that are commonly encountered by a QR code reader.

VI. References

[1] Information technology. Automatic identification and data capture techniques. QR Code 2005 bar code symbology specification.

[2] Querini, Marco, and Giuseppe F. Italiano. "Color Classifiers for 2D Color Barcodes." *IEEE Xplore.*

[3] C.K.P. Clarke. (n.d.). Reed-Solomon error correction. *BBC R&D White Paper*.

[4] Xu, Jun, Lei Zhang, Wangmeng Zuo, David Zhang, and Xiangchu Feng. "Patch Group Based Nonlocal Self-Similarity Prior Learning for Image Denoising." *2015 IEEE International Conference on Computer Vision (ICCV)* (2015).

[5] Chatterjee, P., & Milanfar, P. (2012). Patch-Based Near-Optimal Image Denoising. *IEEE Transactions on Image Processing IEEE Trans. on Image Process., 21*(4), 1635-1649.

[6] Salmon, J., C-A. Deledalle, R. Willett, and Z. Harmany. "Poisson Noise Reduction with Non-local PCA." *2012 IEEE International Conference on Acoustics, Speech and Signal Processing (ICASSP)* (2012).

[7] Liu, Tong, and Xuan Xu. "Quantum Watermarking in M-band Wavelet Domain." *Dongrun-Yau Science Awards (Mathematics)* (2013).

[8] Nguyen, Hieu, and Xiaodi Wang. "Pseudo Quantum Steganography with Pseudo Color Barcode in M-band Wavelet Domain." *Proceeding of 5th International Conference on Applied and Computational Mathematics (ICACM '16)* (2016).

[9] Chang, S., Yu, B., & Vetterli, M. (n.d.). Spatially adaptive wavelet thresholding with context modeling for image denoising. *Proceedings 1998 International Conference on Image Processing. ICIP98 (Cat. No.98CB36269).*

[10] Portilla, J., V. Strela, M.j. Wainwright, and E.p. Simoncelli. "Image Denoising Using Scale Mixtures of Gaussians in the Wavelet Domain." *IEEE Transactions on Image Processing IEEE Trans. on Image Process.* 12.11 (2003): 1338-351.

[11] Lin, Tony, Shufang Xu, Qingyun Shi, and Pengwei Hao. "An Algebraic Construction of Orthonormal M-band Wavelets with Perfect Reconstruction." *Applied Mathematics and Computation* 172.2 (2006): 717-30.

[12] Steffen, P., P.n. Heller, R.a. Gopinath, and C.s. Burrus. "Theory of Regular M-band Wavelet Bases." *IEEE Transactions on Signal Processing IEEE Trans. Signal Process.* 41.12 (1993): 3497-511.

[13] Nielsen, Michael A., and Isaac L. Chuang. "Quantum Information Theory." *Quantum Computation and Quantum Information 10th Anniversary Edition* (n.d.): 528-607.

[14] Verma, Rohit, and Jahid Ali. "A Comparative Study of Various Types of Image Noise and Efficient Noise Removal Techniques." *International Journal of Advanced Research in Computer Science and Software Engineering, 2013.*

[15] SharkD. (2006, October 23). RGBCube b.svg [Image]. Retrieved from https://commons.wikimedia.org/wiki/File:RGBCube_b.svg.

[16] R. (n.d.). Rosistem Barcode - Barcode Education. Retrieved September 20, 2016, from http://www.barcode.ro/tutorials/barcodes/history.html

[17] Lain M.Johnstone and David L Donoho. “Adapting to smoothness via wavelet shrinkage” Journal of the Statistical Association, 90(432):1200–1224, Dec 1995.

[18] S. Mallat “ Wavelet Tour of Signal Processing”. Academic Press, 1998.